

Global investigation of impacts of PET methods on simulating crop-water relations for maize



Wenfeng Liu^{a,*}, Hong Yang^{a,b}, Christian Folberth^{c,d}, Xiuying Wang^e, Qunying Luo^f, Rainer Schulin^g

^a Eawag, Swiss Federal Institute of Aquatic Science and Technology, Ueberlandstrasse 133, CH-8600 Dübendorf, Switzerland

^b Faculty of Sciences, University of Basel, Petersplatz 1, CH-4003 Basel, Switzerland

^c International Institute for Applied Systems Analysis (IIASA), Ecosystem Services and Management Program, Schlossplatz 1, A-2361 Laxenburg, Austria

^d Department of Geography, Ludwig Maximilian University, Munich, Germany

^e Blackland Research and Extension Center, Temple, TX 76502, USA

^f Plant Functional Biology and Climate Change Cluster, University of Technology Sydney, Po Box 123, Broadway 2007, NSW, Australia

^g ETH Zürich, Institute of Terrestrial Ecosystems, Universitätsstr. 16, CH-8092 Zürich, Switzerland

ARTICLE INFO

Article history:

Received 12 October 2015

Received in revised form 13 February 2016

Accepted 21 February 2016

Keywords:

PET

PEPIC

Maize

Crop-water relations

Modelling uncertainties

Global scale

ABSTRACT

Crop models are commonly used to investigate crop-water relations over different spatial scales. Estimating potential evapotranspiration (PET) is a basis for this investigation. Most crop models have built-in PET estimation methods. Using different methods can lead to very different PET estimates; but little is known about the sensitivity of large-scale crop model predictions on the choice of the PET estimation methods. In the work reported here, we used PEPIC, a grid-based EPIC (Environmental Policy Integrated Climate) model with a Python environment, to investigate the impacts of five different PET methods on estimated crop-water relations for maize on a global scale at a resolution of 30 arc min. Results show that the estimated PET varied largely among different PET methods for the same climate zones, leading to uncertainties in estimating crop-water relations. Uncertainties in water-related variables such as growing season evapotranspiration (GSET) and irrigation water requirement were more relevant than uncertainties in crop yields. Water availability played an important role in the uncertainties. All PET methods showed similar performance with respect to simulations of GSET for rainfed maize cultivation in low-rainfall regions, while there were large differences for regions with high rainfall. For irrigated agriculture, the estimated irrigation water requirement varied widely among the five PET methods, with a factor of 2 between the smallest and the largest estimates. Overall, using the Priestley-Taylor method led to lowest yield but highest GSET estimates. The Baier-Robertson and Hargreaves methods produced rather high GSET estimates for tropical and humid regions. The Penman-Monteith method gave the best yield estimates, compared to agricultural statistics. The results highlight the importance of considering the uncertainties resulting from the selection of PET estimation methods in investigating crop-water relations, particularly in predicting impacts of future climate change and in formulating appropriate water management strategies.

© 2016 Elsevier B.V. All rights reserved.

Abbreviations: AET, actual evapotranspiration; APT, actual plant transpiration; ASE, actual soil evaporation; CWP, crop water productivity; CWU, crop water use; EPIC, Environmental Policy Integrated Climate; ET, evapotranspiration; GSET, growing season evapotranspiration; PEPIC, a grid-based EPIC model with a Python environment; PET, potential evapotranspiration; PHU, potential heat units; PPT, potential plant transpiration; PSE, potential soil evaporation.

* Corresponding author.

E-mail addresses: wenfeng.liu@eawag.ch, wfliu2012@gmail.com (W. Liu).

1. Introduction

Agriculture consumes the largest proportion (85%) of global water withdrawals (Shiklomanov, 2003). In the context of climate change and dietary shifts caused by socio-economic development, agriculture is facing the dual challenges of ameliorating water scarcity while increasing crop production (Elliott et al., 2014; Liu et al., 2013). Realistic estimates of global crop water use (CWU) and associated crop production are essential for policy makers to address these challenges.

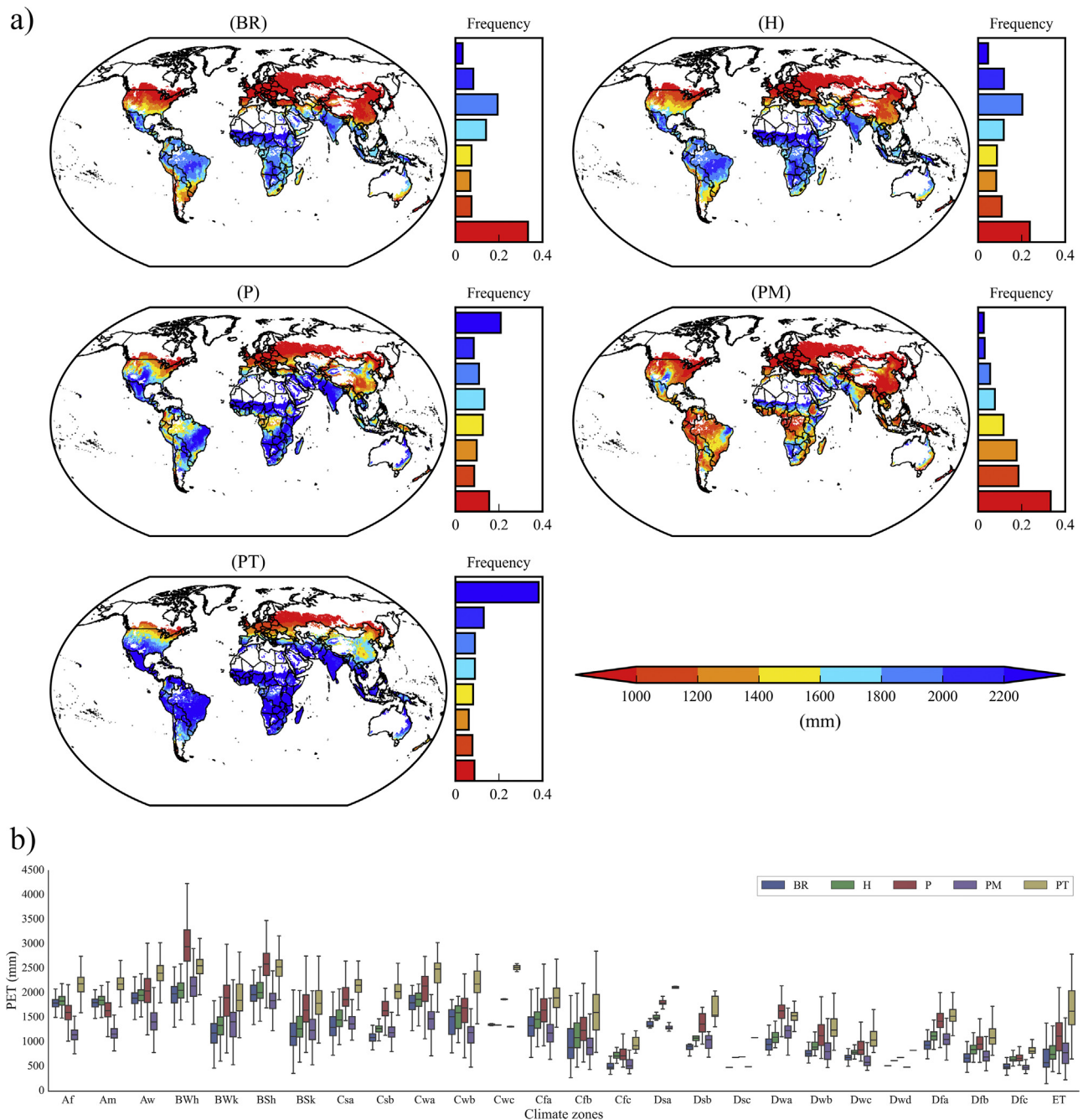


Fig. 1. Spatial patterns of annual potential evapotranspiration (PET) estimates obtained using different PET methods at the (a) grid and (b) Köppen-Geiger levels.

Crop models are increasingly used to project large-scale historical CWU and crop production trends into the future (Elliott et al., 2015; Rosenzweig et al., 2013). There are considerable uncertainties in such predictions, however, originating in particular from inadequate input data, model structure, and parameter estimation methods. There are many studies on how to best identify and reduce these uncertainties in the calibration of these models. Folberth et al. (2013) discussed the impacts of grid resolution on simulating maize yields in America. Liu et al. (2013) and Rosenzweig et al. (2014) investigated the uncertainties relating to future climate change by using different climate data inputs (e.g. General Circulation Models with different climate scenarios). Folberth et al. (2012) explored the influences of potential heat units (PHU) and planting dates on the estimation of maize yields in Sub-Saharan Africa, and the effects of crop management on climate change impact estimates in

the same region (Folberth et al., 2014). Studies addressing similar issues include Balkovič et al. (2014), Xiong et al. (2014) and Yin et al. (2014). However, uncertainties related to the choice of method for the estimation of potential evapotranspiration (PET) have not been assessed and compared in large-scale modelling of CWU and crop production.

PET determines the maximum rate of crop soil water use under conditions of unlimited water availability. An accurate estimation of PET is essential for crop water modelling, since it directly influences the estimation of CWU and irrigation water requirement. It also affects the simulation of crop yields, as crops depend on water to take up nutrients, reduce heat stresses through transpiration, and maintain crop assimilation, among others. Many methods have been introduced to estimate PET (Jensen et al., 1990). We reviewed the PET options in 29 crop models found in the

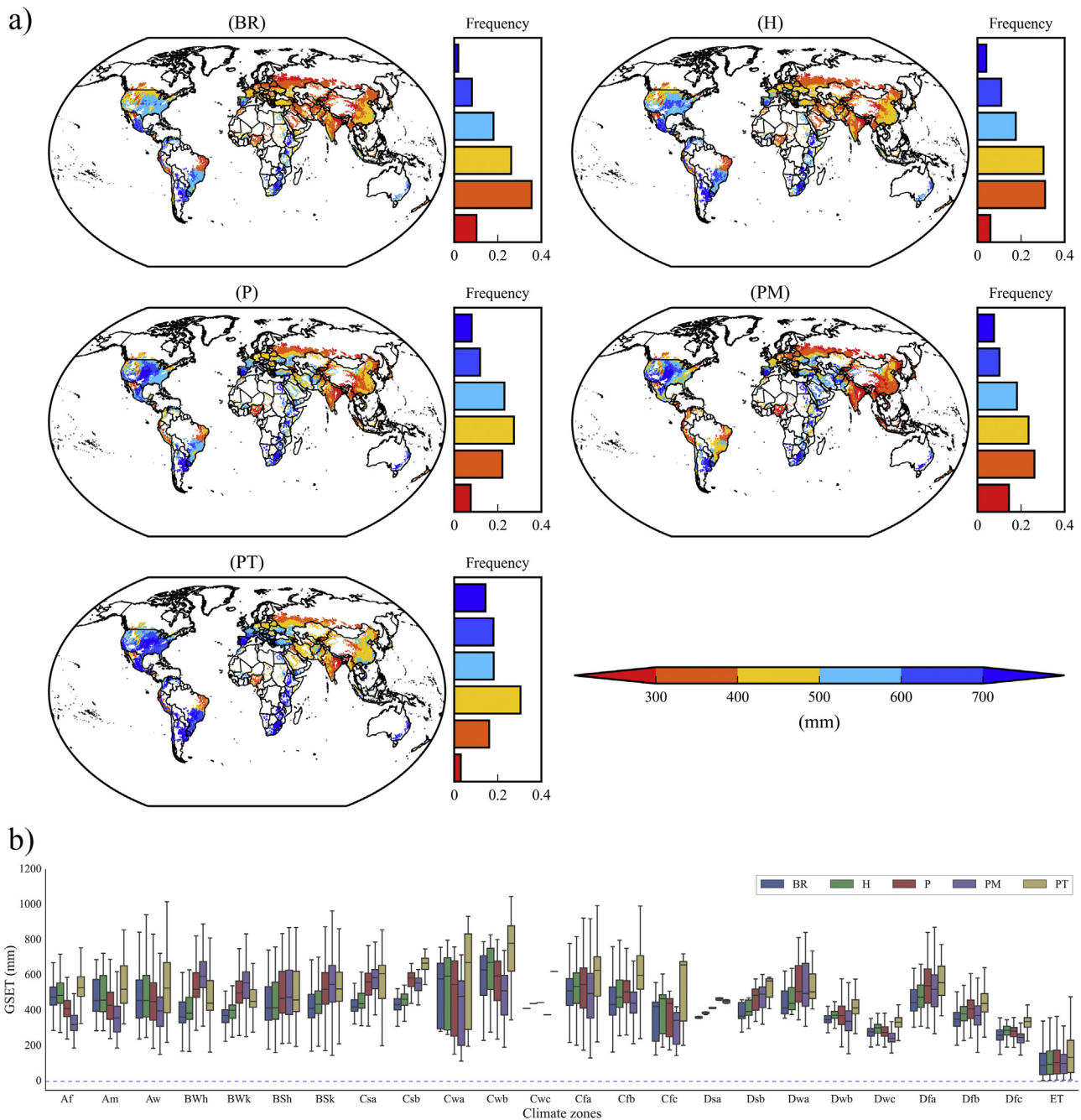


Fig. 2. Spatial patterns of growing season evapotranspiration (GSET) estimates obtained using different PET estimation methods for irrigated maize cultivation at the (a) grid and (b) Köppen-Geiger levels.

literature (Table S1). Often, crop models provide several methodological options to simulate the PET process. For example, five PET methods are available in the EPIC (Environmental Policy Integrated Climate) model (Williams, 1995; Williams et al., 1984), i.e. the Baier-Robertson (BR) (Baier and Robertson, 1965), Hargreaves (H) (Hargreaves and Samani, 1985), Penman (P) (Penman, 1948), Penman-Monteith (PM) (Monteith, 1965), and Priestly-Taylor (PT) (Priestley and Taylor, 1972). The DSSAT (Decision Support System for Agrotechnology Transfer) model provides three of these options: PT, P and PM (Jones et al., 2003). Recently, Palosuo et al. (2011) compared eight crop models for their ability to simulate wheat yields at eight different sites in Europe, while Bassu et al. (2014) analysed 23 crop models for simulating maize yields at four sites across the world. In both studies, the PET methods were

explicitly specified. However, they did not explore the influences of different PET methods on yield estimates. We also reviewed the PET methods used in 20 large-scale crop modelling work (Table S2). Surprisingly, many of them did not specify the PET methods that were employed.

Some earlier studies have shown that different PET estimation methods can have impacts on model results. For instance, Benson et al. (1992) evaluated how the five PET estimation methods in EPIC can influence simulated soil water balances for five locations in America and pointed out the importance of selecting an appropriate PET method. Roloff et al. (1998) assessed how EPIC prediction of wheat yield in a crop rotation experiment field in Canada depended on the method of PET estimation and found that the BR method was the most suitable method. Balkovič et al. (2013) compared the

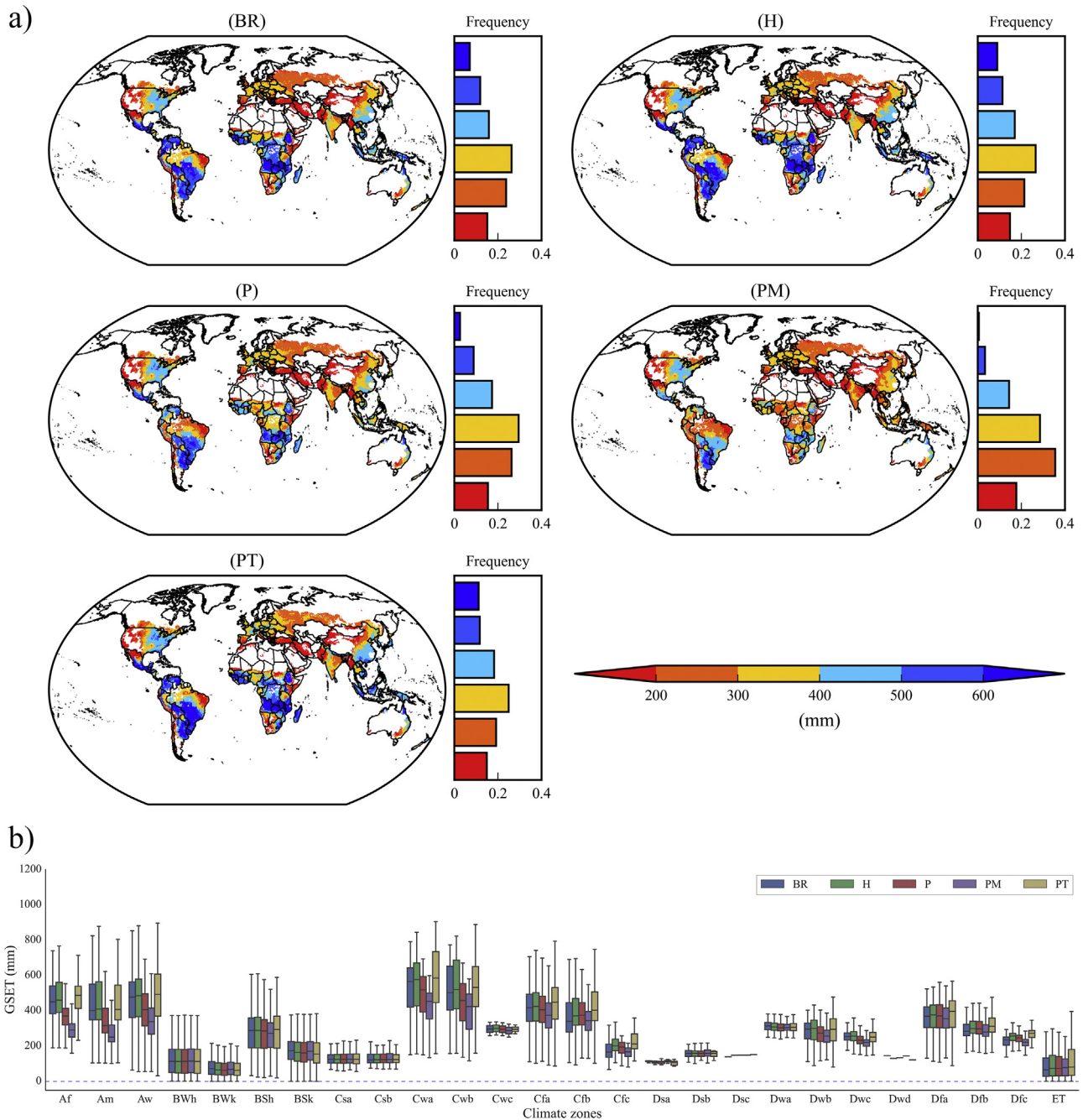


Fig. 3. Spatial patterns of growing season evapotranspiration (GSET) estimates obtained using different PET estimation methods for rainfed maize cultivation at the (a) grid and (b) Köppen-Geiger levels.

performance of the five PET estimation methods in reproducing crop yields in Europe with an EPIC-based model and found that BR and H performed best. [Sau et al. \(2004\)](#) compared the PT, P and some PM-based methods in simulating soil water balances at some sites in Spain using the DSSAT model and concluded that the PM-based methods were the most reliable, while P showed the poorest performance, and PT, though still reasonable, tended to overestimate evapotranspiration (ET). [Anothai et al. \(2013\)](#) compared the PT and PM methods in combination with the DSSAT model for an experimental site in Colorado, USA, and also found PM to perform better than PT. These studies show how important a proper choice of the PET estimation methods is and that this choice depends on site, especially climate conditions. To be able to make an informed choice it is of significance to know from where the uncertainties

in different PET methods come and for which conditions various methods perform best. However, previous works comparing different PET methods were mostly conducted on regional scale and focused on either yields or crop soil water use. Such kind of research is rare for large-scale simulations. A comprehensive assessment of impacts of different PET estimation methods on crop yields and water use in rainfed and irrigated systems on a global scale with specification of climate zones has been absent.

EPIC is one of the most widely used crop models ([Balkovič et al., 2013](#); [Folberth et al., 2012, 2014](#); [Liu et al., 2007](#); [Tan and Shibasaki, 2003](#)) due to its good performance in a large variety of applications throughout the world ([Gassman et al., 2005](#)). The five PET estimation methods offered in EPIC were developed for applications in different climate regions and for different situations of climate data

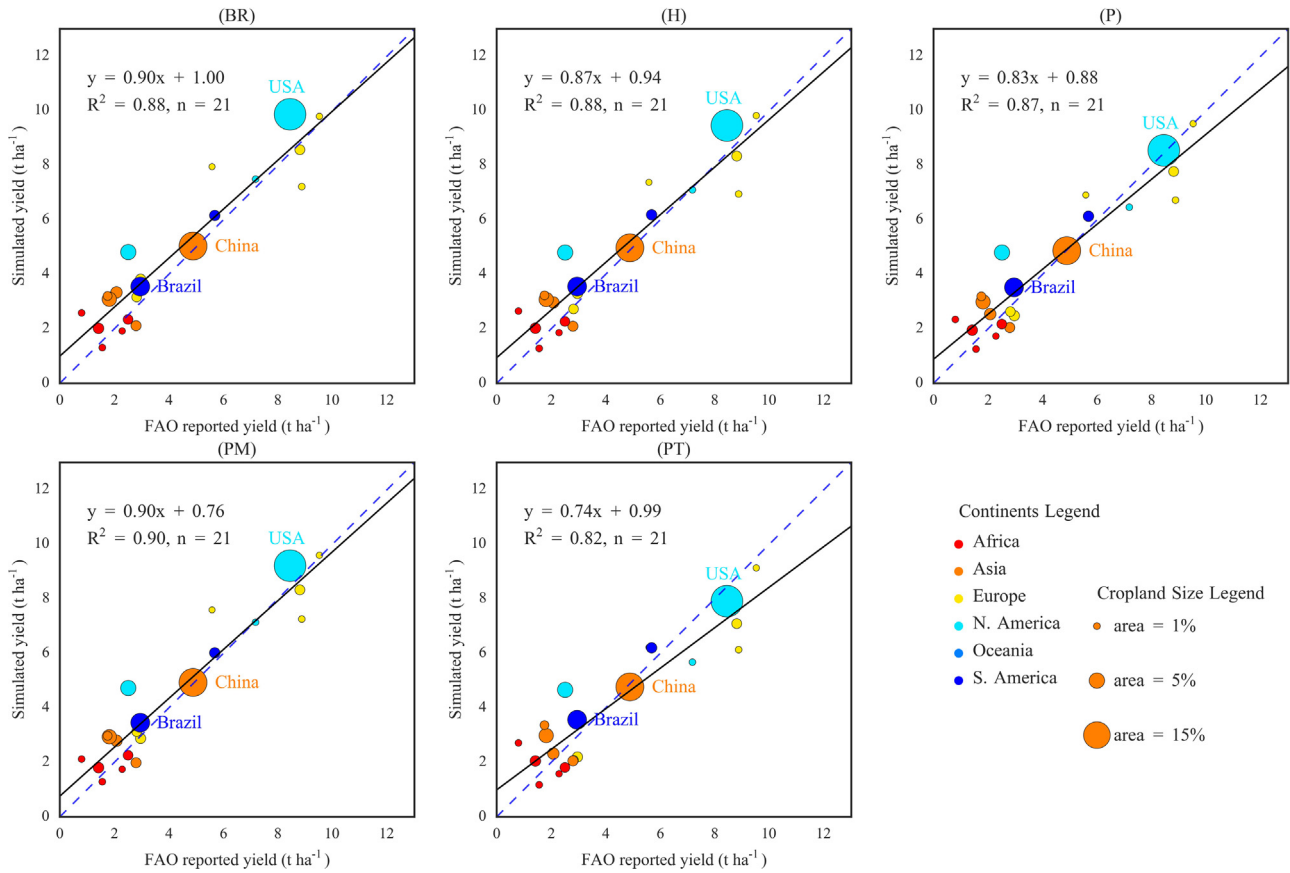


Fig. 4. Comparisons between reported and estimated yields using different PET estimation methods for major maize-producing countries. Colours represent continents, and the areas of the circles represent the areas of land used for maize production in the respective countries relative to the total area used for maize cultivation worldwide.

availability. The H method was often used for large-scale simulations in cases of limited climate data availability (Folberth et al., 2013; Liu, 2009; Liu et al., 2013). However, after global gridded climate datasets (e.g. Hempel et al. (2013); Elliott et al. (2015)) have become available recently, it is now possible also to use the other PET estimation methods in large-scale simulations with EPIC.

Here, we used PEPIC, a grid-based EPIC model with a Python environment, to compare how the choice of the PET estimation methods would influence global scale simulations of maize growth and to identify error sources for different climate zones. In addition to PET, we analysed growing season evapotranspiration (GSET), yields, CWU, crop water productivity (CWP), and total maize production, which are all related to PET. To our best knowledge, this is the first study exploring the influences of PET estimation methods on simulating crop growth and water consumption on a global scale.

2. Simulation framework

2.1. Methodologies

2.1.1. The EPIC model and PET methods

The EPIC model was initially introduced by Williams et al. (1984) to evaluate the impacts of soil erosion on soil productivity. Since its first release, it has been continuously improved and expanded by integrating some major components from other models, such as CREAMS (Knisel, 1980), GLEAMS (Leonard et al., 1987), Century (Parton et al., 1994), and ALMANAC (Kiniry et al., 1992). EPIC can be used to simulate a large number of complex soil, water, climate, crop development and agricultural management processes (Williams et al., 1984). EPIC simulates crop growth at a daily step

based on the concept of energy-biomass conversion. Daily potential biomass increase is the product of intercepted solar radiation and a crop-specific biomass-energy ratio. The potential increase in biomass is reduced each day in response to the dominating plant stress (water, nutrient, temperature, aeration, and salinity) to obtain the actual biomass. The crop yield is estimated by the product of the harvest index and actual biomass accumulation (Williams, 1995).

In EPIC, PET can be calculated using one of the following five functions:

$$PET_{BR} = 0.288 \times T_{max} - 0.144 \times T_{min} + 0.139 \times RAMX - 4.931 \quad (1)$$

$$PET_H = 0.0032 \times \left(\frac{RAMX}{(2.501 - 0.0022 \times T)} \right) \times (T + 17.8) \times (T_{max} - T_{min})^{0.6} \quad (2)$$

$$PET_P = \left(RN \times \delta / (2.501 - 0.0022 \times T) + \gamma \times (2.7 + 1.63 \times U) \right) \times EA(1 - RH) / (\delta + \gamma) \quad (3)$$

$$PET_{PM} = \left(RN \times \delta + 86.66 \times AD \times EA(1 - RH) \times U / 350 \right) / \left((2.501 - 0.0022 \times T) \times (\delta + \gamma) \right) \quad (4)$$

$$PET_{PT} = 1.28 \times \left(RN \times (1.0 - AB) / (2.501 - 0.0022 \times T) \right) \times \left(\delta / (\delta + \gamma) \right) \quad (5)$$

where PET_{BR} , PET_H , PET_P , PET_{PM} , and PET_{PT} are the PET [mm d^{-1}] estimates obtained by using the BR, H, P, PM and PT methods, respectively; T_{\max} and T_{\min} are the daily maximum and minimum temperatures [$^{\circ}\text{C}$]; $RAMX$ is the clear day solar radiation at the surface [$\text{MJ m}^{-2} \text{d}^{-1}$] and can be calculated based on day of the year and latitude; T is the daily mean air temperature [$^{\circ}\text{C}$]; RN is the net radiation [$\text{MJ m}^{-2} \text{d}^{-1}$]; δ is the slope of the saturation vapour pressure curve [$\text{kPa } ^{\circ}\text{C}^{-1}$]; γ is the psychrometer constant [$\text{kPa } ^{\circ}\text{C}^{-1}$]; U is the daily mean wind speed [m s^{-1}]; EA is the saturation vapour pressure at mean air temperature [kPa]; RH is the daily mean relative humidity; AD is the air density [Kg m^{-3}]; and AB is the soil albedo.

With P, PT, H and BR, potential plant transpiration (PPT) is estimated by using an approach similar to Ritchie (1972) as following:

$$\begin{cases} PPT = PET \times LAI/30 \leq LAI \leq 3 \\ PPT = PETLAI > 3 \end{cases} \quad (6)$$

where LAI is the leaf area index. With PM, PPT is calculated as:

$$PPT = (RN \times \delta + 86.66 \times AD \times EA(1 - RH)/AR) / ((2.501 - 0.0022 \times T) \times (\delta + \gamma(1 + CR/AR))) \quad (7)$$

where AR is the aerodynamic resistance for heat and vapour transfer [s m^{-1}]; CR is the canopy resistance for vapour transfer [s m^{-1}], which can be calculated as:

$$CR = p_1 / (LAI \times g_0 \times (1.4 - 0.00121 \times CO_2)) \quad (8)$$

where P_1 is a parameter used in EPIC to adjust PPT estimation ranging between 1.0 and 2.0 and a default value of 1 was used in this study; g_0 is the leaf conductance [m s^{-1}] and CO_2 is the carbon dioxide concentration [ppm].

Potential soil evaporation (PSE) is calculated as:

$$PSE = \max \{ (PET - I) \times SCI, 0 \} \quad (9)$$

where I is the rainfall interception [mm d^{-1}]; SCI is a soil cover index varying between 0 and 1, which can be calculated as:

$$SCI = \exp \{ -\max(0.4 \times SMLA, 0.1 \times (CV + 0.1)) \} \quad (10)$$

where $SMLA$ is the sum of the LAI and CV is the weight of all above ground plant material [t ha^{-1}]. When $PET < I$, both actual plant transpiration (APT) and soil evaporation (ASE) are set to 0. Otherwise, they are estimated as:

$$APT = \min \{ (PET - I), PPT \} \quad (11)$$

$$ASE = \min \{ PSE, PSE \times (PET - I) / (PSE + APT) \} \quad (12)$$

Actual evapotranspiration (AET) is the sum of APT and ASE. The climate variables required as input for each PET method are listed in Table 1.

2.2. The PEPIC model

PEPIC runs the EPIC (the latest version v0810) model within a Python-based framework. The whole study domain is firstly categorized into a number of subareas depending on the study purposes

(e.g. administrative boundaries, climate regions, watersheds). Input data (e.g. elevation, slope, climate, soil, and management practice information) need to be specified for each grid cell, which has a spatial resolution of 30 arc min. After simulation is complete for all grids cells, PEPIC extracts the results and presents the spatial distribution of desired variables for a given time period. In this study, we simulated crop growth processes separately for irrigated and rainfed maize cultivation. To get combined outputs for each grid cell, values from irrigated and rainfed cultivation were aggregated using area-weighted averaging as described by Liu et al. (2007).

2.3. Data description

The input data for the PEPIC model include latitude, longitude, elevation, slope, climate, soil properties, nitrogen and phosphorus fertilizer as well as irrigation application rates, cropland use areas for irrigated and rainfed cultivation, planting dates, harvesting dates, and PHU.

Climate data required to run PEPIC include solar radiation, maximum and minimum air temperature, precipitation, relative humidity, wind speed, and CO_2 concentration. In this study, the Global Annual Mean CO_2 Dataset provided by Goddard Institute for Space Studies (GISS) of National Aeronautics and Space Administration (NASA) was used. The other climate variables were obtained from the Global Gridded Crop Model Intercomparison (GGCMI) Project (Elliott et al., 2015). This dataset is based on WFDEI (Weedon et al., 2014) ERA-Interim historical re-analysis data that have been bias corrected on a monthly scale against the Climate Research Unit (CRU) data (Mitchell and Jones, 2005). It spans the time period of 1979–2012, which is also the simulation period in this study. Soil properties of layer depth, pH, bulk density, organic carbon content, % sand, and % silt, etc. were extracted from the ISRIC-WISE (Batjes, 2006). This soil dataset was spatially linked to the FAO Digital Soil Map (FAO, 1995).

The fertilizer application rates of N and P around 2000 were derived from the FertiStat (FAO, 2007). This dataset is only available at the country level. Application rates were assumed to be the same for the different grid cells within a given country in this study. Because of the available data on irrigation rates were not sufficiently complete, an automatic irrigation schedule with a maximum total volume of 1000 mm for the whole growing season was employed to guarantee enough water for crop growth. Besides, the minimum and maximum single application volumes were set to 1 and 500 mm. This kind of irrigation strategy is commonly assumed in large scale crop modelling (Rosenzweig et al., 2014). Harvested maize areas for irrigated and rainfed cultivation were obtained from the MIRCA2000 dataset (Portmann et al., 2010), which provides the irrigated and rainfed areas for 26 crops within the period of 1998–2002.

The required data on planting dates and harvesting dates were obtained from the Center for Sustainability and the Global Environment (SAGE) (Sacks et al., 2010). The SAGE dataset includes the beginning, medium, end of planting/harvesting dates for 19 crops. Medium values were used in our study. PHU was calculated by using the PHU Calculator of the Blackland Research Center

Table 1
Description of potential evapotranspiration (PET) methods and associated climate variables.

Method	Abbreviation	Solar radiation (RN)	Temperature (T, T_{\min} , T_{\max})	Relative humidity (RH)	Wind speed (U)	Reference
Baier-Robertson	BR		Yes			Baier and Robertson (1965)
Hargreaves	H		Yes			Hargreaves and Samani (1985)
Penman	P	Yes	Yes	Yes	Yes	Penman (1948)
Penman-Monteith	PM	Yes	Yes	Yes	Yes	Monteith (1965)
Priestley-Taylor	PT	Yes	Yes			Priestley and Taylor (1972)

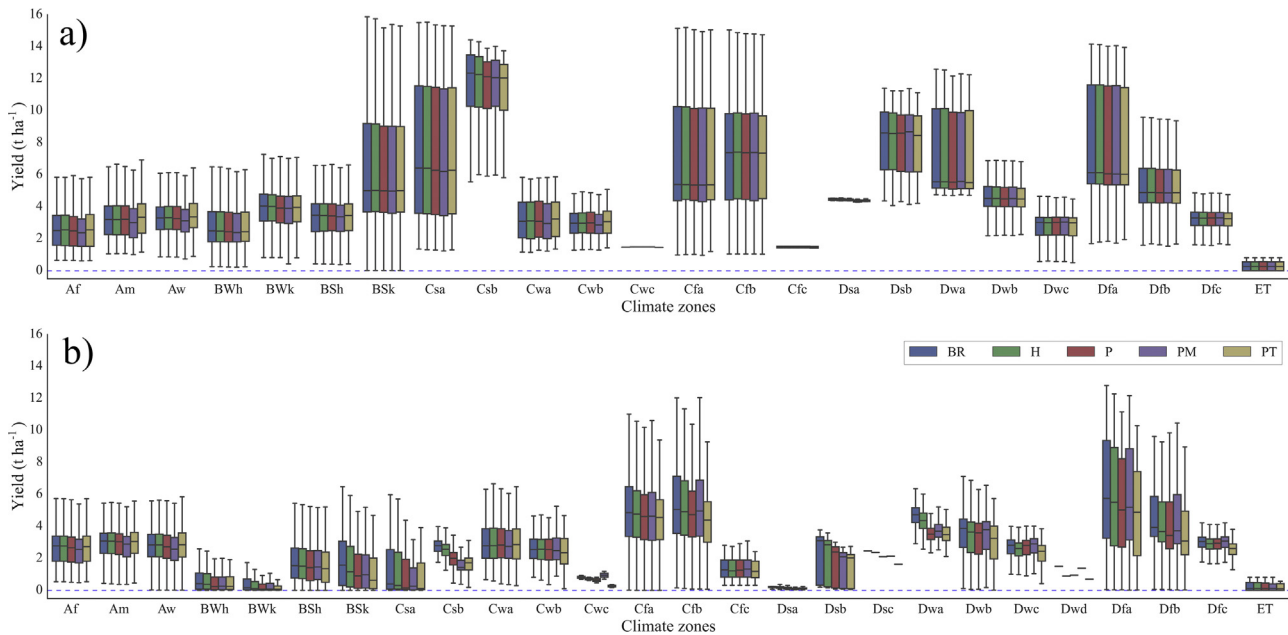


Fig. 5. Simulated maize yields at the Köppen-Geiger level for (a) irrigated and (b) rainfed cultivation.

based on the input data of planting dates, harvesting dates and temperature.

Besides the grid-based analyses, also an updated version of the Köppen-Geiger classification of climate zones (Peel et al., 2007) was used to compare the results. The Köppen-Geiger classification divides the whole world into five major categories (Table 2), i.e. A (tropical), B (arid), C (temperate), D (cold) and E (polar) based on global temperature and precipitation information. Details about the Köppen-Geiger classification can be found at <http://www.hydrol-earth-syst-sci.net/11/1633/2007/hess-11-1633-2007-supplement.zip>. The Köppen-Geiger classification has been widely used as a basis for regionalisation of climatic variables such as in GGCM (Elliott et al., 2015). Table 2 shows the climate zones and the irrigated and rainfed maize areas in each zone.

2.4. Description of estimated variables

GSET is the accumulated AET from planting date to harvesting date. Irrigation is automatically triggered when water stress factor (ratio between daily plant water use and daily potential water use) is lower than 0.9. Irrigation rate is determined by the minimum of the maximum single application volume and the volume required to fill the soil moisture to field capacity. Irrigation water requirement in this study is defined as the total applied irrigation rates during the whole growing season for irrigated maize cultivation. CWU was calculated by multiplying GSET with crop harvest areas at the grid cell level and then summing over all grid cells. For irrigated cultivation, CWU was separated into blue and green CWU, where green CWU refers to the CWU derived from soil moisture and precipitation, while blue CWU is the CWU originating from irrigation. We adopted the methods introduced in Liu et al. (2009) to separate blue and green CWU. Crop water productivity (CWP) is defined as the ratio between maize yield and GSET (Liu et al., 2007). For consistency with MIRCA2000 data and fertilizer inputs, results in this study were averaged between 1998 and 2002.

3. Results

3.1. Estimation of potential evapotranspiration (PET)

The five PET estimation methods compared here produced quite different annual PET distributions (Fig. 1a). Only H and BR gave similar results. With H more grid cells fell into the high range (>2000 mm) than with BR, while with BR more cells fell into the low range (<1000 mm). Major differences were found among PM, P and PT methods. The PM method produced a large fraction of low values (<1000 mm) and the smallest fraction of high values (>1600 mm), whereas estimates obtained with P and PT were dominated by high values (>1600 mm). With PT more than half of all grid cells had annual PET values >2000 mm. The largest differences were found for the tropical and arid regions, southwestern part of America, Mexico, and southeastern part of China.

Large differences in estimated annual PET were also evident at the level of the Köppen-Geiger climate zones (Fig. 1b). The lowest annual PET values were obtained with the PM method for the Af, Am, Aw, Cwa, Cwb, Cfa, Cfb and Cfc zones. For other zones, BR estimated the lowest annual PET values. In contrast, PT estimates were the highest in all Köppen-Geiger zones except in the arid regions Bwh, BWk and BSh, where P gave the highest values. As for the grid cells, the H method produced a similar pattern to that of BR, but with higher values. Different climate variables used in different PET estimation methods contribute to the variations in PET estimations in a given climate zone. For example, the P and PM methods consider relative humidity and wind speed in PET estimation, which are not considered in the other PET methods.

3.2. Estimation of growing season evapotranspiration (GSET)

3.2.1. Irrigated maize cultivation

Generally, the differences in GSET estimates (Fig. 2) obtained with the different PET estimation methods were smaller than those shown in PET values (Fig. 1). This is because GSET is also related to other crop growth factors, especially the development of LAI. The PT method produced higher GSET values than the other PET methods, as shown with more grid cells falling into the range of >600 mm

Table 2
Definition of the Köppen-Geiger climate zones and harvest areas in irrigated and rainfed systems of maize.

Zone	Definition	Irrigated		Rainfed		Combined		Percent of irrigated and rainfed area in each zone	
		Harvest area (ha)	Percent in the total irrigated area (%)	Harvest area (ha)	Percent in the total rainfed area (%)	Harvest area (ha)	Percent in the total mixed area (%)	Irrigated (%)	Rainfed (%)
Af	Tropical rainforest	123,627	0.43	3,820,347	3.23	3,943,974	2.68	3.13	96.87
Am	Tropical monsoon	253,565	0.87	3,881,438	3.28	4,135,003	2.81	6.13	93.87
Aw	Tropical Savannah	1,326,765	4.56	24,270,654	20.53	25,597,419	17.38	5.18	94.82
BWh	Arid desert hot	1,387,463	4.77	328,925	0.28	1,721,057	1.17	80.62	19.11
BWk	Arid desert cold	910,677	3.13	44,427	0.04	956,655	0.65	95.19	4.64
BSh	Arid steppe hot	1,075,022	3.70	4,072,646	3.44	5,147,970	3.49	20.88	79.11
BSk	Arid Steppe cold	1,722,430	5.92	624,599	0.53	2,347,029	1.59	73.39	26.61
Csa	Temperate dry and hot summer	182,738	0.63	69,399	0.06	252,212	0.17	72.45	27.52
Csb	Temperate day and warm summer	78,896	0.27	21,706	0.02	100,602	0.07	78.42	21.58
Cwa	Temperate dry winter and hot summer	304,081	1.05	2,215,906	1.87	2,519,987	1.71	12.07	87.93
Cwb	Temperate dry winter and warm summer	42,648	0.15	1,300,172	1.10	1,342,820	0.91	3.18	96.82
Cwc	Temperate dry winter and cold summer	6	0.00	1116	0.00	1122	0.00	0.53	99.47
Cfa	Temperate no dry season hot summer	7,458,669	25.65	22,468,226	19.00	29,927,094	20.32	24.92	75.08
Cfb	Temperate no dry season warm summer	1,879,087	6.46	9,527,090	8.06	11,406,177	7.74	16.47	83.53
Cfc	Temperate no dry season cold summer	3855	0.01	3179	0.00	7034	0.00	54.81	45.19
Dsa	Cold dry and hot summer	1447	0.00	1483	0.00	2930	0.00	49.39	50.61
Dsb	Cold dry and warm summer	2878	0.01	956	0.00	3834	0.00	75.07	24.93
Dsc	Cold dry and cold summer	0	0.00	30	0.00	30	0.00	0.00	100.00
Dwa	Cold dry winter and hot summer	987,116	3.39	1,214,479	1.03	2,201,595	1.49	44.84	55.16
Dwb	Cold dry winter and warm summer	804,639	2.77	866,153	0.73	1,670,792	1.13	48.16	51.84
Dwc	Cold dry winter and cold summer	93,082	0.32	164,158	0.14	257,240	0.17	36.18	63.82
Dwd	Cold dry winter and very cold summer	0	0.00	7	0.00	7	0.00	0.00	100.00
Dfa	Cold no dry season hot summer	8,954,943	30.79	27,410,705	23.19	36,365,648	24.69	24.62	75.38
Dfb	Cold no dry season warm summer	1,425,208	4.90	15,598,072	13.19	17,023,280	11.56	8.37	91.63
Dfc	Cold no dry season cold summer	44,914	0.15	281,278	0.24	326,192	0.22	13.77	86.23
ET	Polar tundra	19,102	0.07	37,535	0.03	56,637	0.04	33.73	66.27

Table 3
Comparison of global aggregated crop water use (CWU, in 10^9 m^3), crop production (in 10^6 t), and crop water productivity (CWP, in kg m^{-3}) for maize based on different PET methods in the EPIC model and comparison with literatures.

Variable	This study					Chapagain and Hoekstra (2004) Fader et al. (2011) Mekonnen and Hoekstra (2011) Siebert and Döll (2010)			
	BR	H	P	PM	PT	PM	PT	PM	PM
Irrigated blue CWU	35.68	40.98	55.81	53.19	60.35		66.38	51	72.4
Irrigated green CWU	94.01	94.86	92.70	88.29	98.45			104	
Rainfed CWU	498.29	512.33	486.32	442.90	537.86			493	
Total CWU	627.97	648.17	634.83	584.37	696.67	548.39	592.67	648	657.7
Irrigated production	186.57	187.04	185.16	184.25	185.56				
Rainfed production	610.63	588.23	545.47	573.73	512.47				
Mixed production	797.21	775.29	730.66	757.99	698.06				
Irrigated CWP	1.44	1.38	1.25	1.30	1.17			1.125	
Rainfed CWP	1.23	1.15	1.12	1.29	0.95			0.924	
Combined CWP	1.27	1.20	1.15	1.30	1.00	1.1		0.973	0.919

and few grid cells falling into the range of $<300 \text{ mm}$ GSET (Fig. 2a). In contrast, the BR and H methods gave relatively low GSET values, with more grid cells falling into the range of $<400 \text{ mm}$ and less grid cells into the range of $>700 \text{ mm}$ than with the other methods. The PM and P produced comparable spatial patterns and frequency distributions of grid cells. Also at the Köppen-Geiger level, the variation of GSET estimates was not as significant as in PET estimates (Figs. 1b and 2b). The PT method resulted in the highest GSET for all regions, with the exception of Bwh, Bwk, Bsh and BSk, where the PM method led to the highest values. On the other hand, PM produced low values in many other regions, especially in the Af, Am, Aw, Cwa, Cwb, Cfa, Cfb and Cfc regions. BR and H showed again similar performance with low GSET estimates especially for arid and cold regions and high GSET estimates for the Af, Am, Aw, Cwa, Cwb, and Cfc regions (Fig. 2b).

3.2.2. Rainfed maize cultivation

The differences among GSET estimates obtained with the five PET estimation methods were relatively small also for rainfed maize cultivation (Fig. 3). Rather large differences only occurred between PM and PT estimates (Fig. 3a). PM resulted in low GSET values ($<300 \text{ mm}$) for the majority of grid cells ($>50\%$), while PT produced much higher values ($>500 \text{ mm}$) for most grid cells. Furthermore, PT, H and BR methods led to high GSET values for tropical regions, in contrast to P and PM. At the Köppen-Geiger level, similar GSET values were obtained with all the five PET estimation methods except for the Af, Am, Aw, Cwa, Cwb, Cfa, Cfb and Cfc regions (Fig. 3b). In the latter eight regions, PT, H and BR estimates of PET produced higher GSET values than the other two methods, while PM estimates produced the lowest GSET values.

3.3. Estimation of maize yields

The performance of different PET methods was evaluated against the reported yields for individual countries. Country-specific reported yield data were downloaded from FAO (Food and Agriculture Organization of the United Nations) database (<http://faostat3.fao.org/home/E>). For consistency with the estimated yields, FAO reported yields were also averaged for 1998 and 2002. Generally, the PEPIC model performed well in estimating yields for all the countries by using the five PET methods (Fig. S1). However, biases can be found for minor maize producers. In order to show the overall trends more clearly, Fig. 4 presents the respective results only for the 21 major maize producing countries, i.e. the countries with cropland area used for maize cultivation larger than 0.8% of the global total maize cultivation areas. These 21 countries account for more than 80% of the global areas used for maize production. The slopes of the regression lines between estimated and reported maize yields were 0.90, 0.87, 0.83, 0.90, and 0.74 for the simulations based on PET estimation with the BR, H, P, PM,

and PT methods, respectively. The slopes for P and PT were significantly different from 1 at the 95% statistical level. The intercepts of the regression lines were 1.00, 0.94, 0.88, 0.76, and 0.99 (all significantly different from 0 at the 95% statistical level), respectively, and the R^2 values ranged between 0.82 and 0.90, demonstrating that PEPIC performed relatively well in estimating maize yields for the major maize-producing countries.

The best performance (large slope and R^2 , low intercept) of the five PET estimation methods was found for PM, but BR and H performed almost as well, while the poorest performance was found for PT (Fig. 4). Using PT, PEPIC tended to underestimate high yields (e.g. $>6 \text{ t ha}^{-1}$) more than using the other PET estimation methods. The differences in yield estimates related to the choice of the PET estimation method mainly resulted from differences in yield simulations for rainfed maize cultivation, while there was little variation related to the PET estimation methods for irrigated maize cultivation (Fig. 5 and Fig. S2). Also in rainfed maize cultivation there were only small differences relating to PET estimation for regions of Af, Am, Aw, Cwa, Cwb, and Cfc, whereas differences were more notable for regions of such as Csa, Csb, Dwa, Dfa, and Dfb (Fig. 5b).

3.4. Estimation of irrigation water requirement and crop water productivity (CWP)

The highest irrigation water requirement occurred in the regions of BWh, BWk, BSh and BSk, Csa, and Csb (Fig. 6). For regions with generally high irrigation demand, the BR and H methods of PET estimation generally predicted the lowest demand. On the other hand, the PT method with few exceptions tended to predict the highest irrigation water requirement.

In most cases BR estimation of PET resulted in the highest CWP values for irrigated maize cultivation (Fig. 7a). Only in the tropical areas (Af, Am, Aw) and in the Cwa, Cwb, Cfa, Cfb and Cfc regions the highest values were produced using the PM method. On the other hand, PT method produced the lowest values except for the arid areas (BWh, BWk, BSk and BSk) and for Csa and Dsb, where PM led to the lowest CWP estimates. The patterns for rainfed maize were similar to the irrigated system (Fig. 7b).

3.5. Global aggregated CWU, production and CWP

Using PT to estimate PET produced the highest total CWU in both irrigated ($158.80 \times 10^9 \text{ m}^3$) and rainfed ($537.86 \times 10^9 \text{ m}^3$) maize cultivation, while PM produced the lowest total CWU ($442.90 \times 10^9 \text{ m}^3$) for rainfed cultivation and BR the lowest total CWU ($129.68 \times 10^9 \text{ m}^3$) for irrigated cultivation (Table 3). When separating the total CWU for irrigated cultivation into blue and green CWU, the PM method produced the lowest green CWU ($88.29 \times 10^9 \text{ m}^3$), while BR resulted in the lowest blue CWU

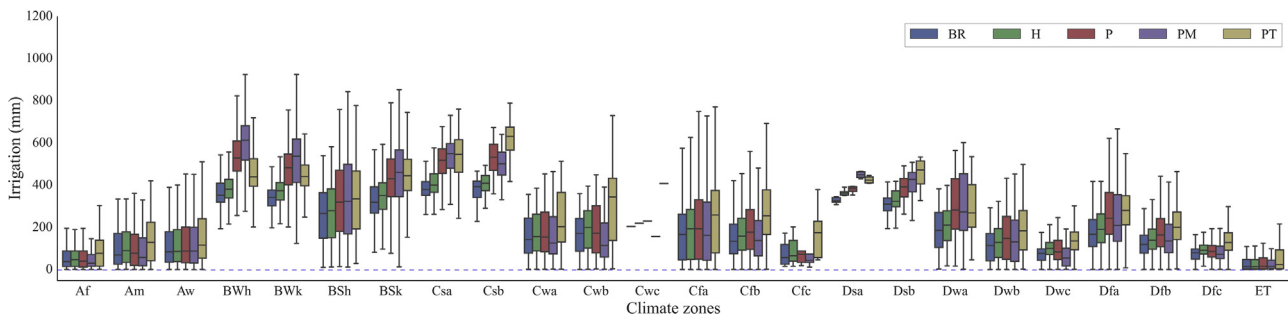


Fig. 6. Simulated irrigation water requirement at the Köppen-Geiger level.

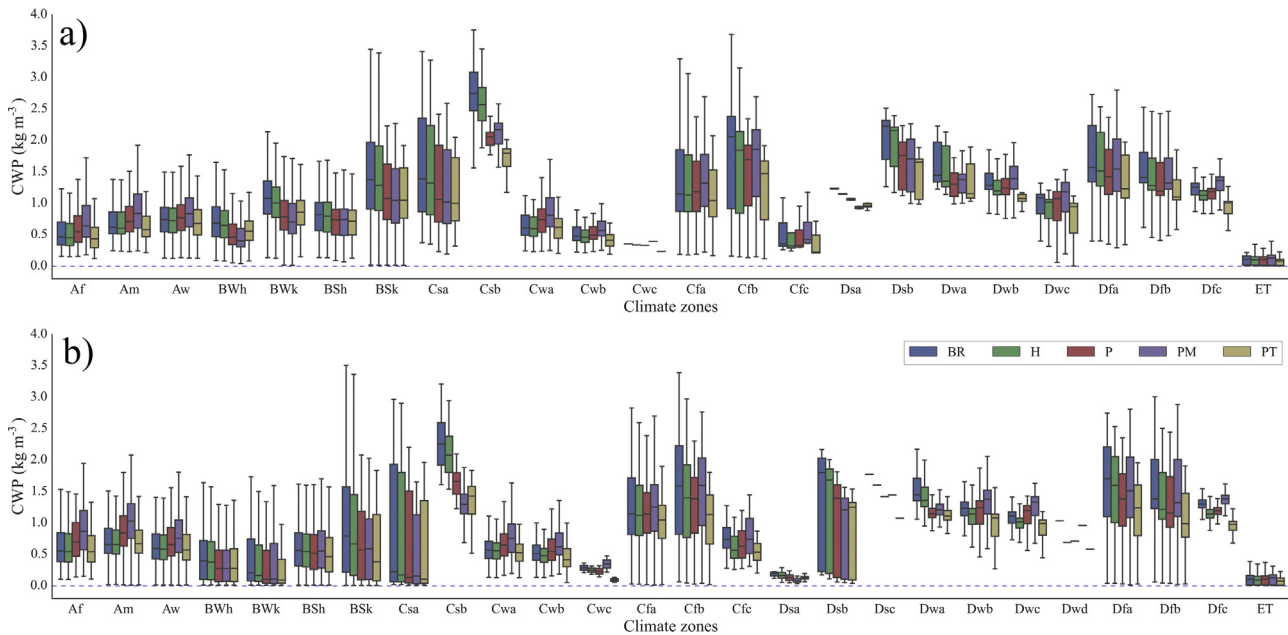


Fig. 7. Simulated (a) irrigated and (b) rainfed maize crop water productivity (CWP) at the Köppen-Geiger level.

($35.68 \times 10^9 \text{ m}^3$). Also for rainfed and irrigated cultivation combined, the PM-based CWU estimates were the lowest.

In accordance with the results for the yields, the estimates of total rainfed maize production were quite sensitive to the choice of the PET estimation methods, while there was little sensitivity for irrigated maize production (Table 3). PT gave the lowest ($512.47 \times 10^6 \text{ t}$) and BR the highest ($610.63 \times 10^6 \text{ t}$) estimates for rainfed maize production. For irrigated maize, H-based simulation estimated the highest and PM-based simulations the lowest production, but the difference between them was only $2.8 \times 10^6 \text{ t}$. The estimates of global total maize production for both systems combined decreased with the choice of PET estimation methods in the order BR, H, PM, P, PT. The difference of $99.15 \times 10^6 \text{ t}$ between maximum and minimum productions was almost equivalent to China's total maize production in 2000 ($106 \times 10^6 \text{ t}$).

The estimated global average CWP varied between 1.17 and 1.44 kg m^{-3} for irrigated maize cultivation and between 0.95 and 1.29 kg m^{-3} for rainfed maize cultivation (Table 3). While the lower bounds of these range resulted from PET estimates based on the PT method in both cases, the upper value resulted for irrigated production from using the BR method and for rainfed production from using the PM method.

4. Discussion

4.1. Comparison of CWU and CWP with other studies

The green CWU of maize was two times the blue CWU for irrigated maize cultivation in the study of Mekonnen and Hoekstra (2011). Our study obtained similar results with much higher green CWU than blue CWU for irrigated maize (Table 3). Total volumes of blue CWU in global irrigated maize production reported in the literatures varied between 51×10^9 and $72.4 \times 10^9 \text{ m}^3$ (Fader et al., 2011; Mekonnen and Hoekstra, 2011; Siebert and Döll, 2010). Our estimates of blue CWU by using P, PM and PT for estimating PET were within this range, while the estimates based on BR and H methods were lower. The total CWU for maize production was previously reported to range between 548.39×10^9 and $657.7 \times 10^9 \text{ m}^3$ (Chapagain and Hoekstra, 2004; Fader et al., 2011; Mekonnen and Hoekstra, 2011; Siebert and Döll, 2010). The estimates obtained in this study were all within this range, except for the PT method, which tended to overestimate CWU. Ranging between 1.00 and 1.30 the CWP values estimated in this study were of the same magnitude as the value estimated by Chapagain and Hoekstra (2004), but higher than the values estimated by Mekonnen and Hoekstra (2011) and Siebert and Döll (2010).

4.2. Influences of water availability on GSET and yield estimates

For irrigated maize cultivation, the variation of GSET estimates was considerable with PET estimation methods in all climate regions. However, the variation of GSET estimates presented different patterns at the Köppen-Geiger level for rainfed maize cultivation, with high variation in some regions (e.g. Af, Am, Aw, Cwa, Cwb, Cfa, Cfb, and Cfc), but quite low variation in the other regions (Fig. 3b). This is mainly due to the influence of the spatial pattern of annual precipitation. We found that the average annual precipitation in the aforementioned eight climate regions was greater than 800 mm, especially in the tropical areas (Fig. S3). High annual precipitation leads to less limit on GSET in these regions. However, the GSET estimates were strongly constrained by water availability in the rainfall limited regions, leading to low variation. This finding is consistent with Wang and Dickinson (2012). It suggests the important role of water availability on the variation of GSET estimation with different PET methods.

The yield estimates showed little variation with PET estimation methods for irrigated maize cultivation (Fig. 5a). This is mainly attributable to the fact that irrigation was set automatically to a level that is sufficient for crop needs in PEPIC independent of PET estimation methods. The major differences of yield estimates were found in the limited water availability regions for rainfed maize cultivation (Fig. 5b), especially for the regions of Dfa and Dfb, which had high fractions of total rainfed cropland areas (Table 2). This is because the effects of PET methods on yields will only show up when water availability is limited. Consequently, the global total maize production varied largely for rainfed maize cultivation (Table 3).

4.3. Assessment of the performance of different PET methods

In this study, the PT method produced the highest annual PET estimates, and consequently also the highest GSET estimates for both irrigated and rainfed maize cultivation and the lowest maize yield estimates for rainfed maize. Also the PT method tends to underestimate yields for high-yield countries (compared with the reported yields) (Fig. 4 and Fig. S1). The main reason for underestimating yields may be related to its overestimation of water stress (Fig. S4) stemmed from overestimation of PET.

The BR method was developed in Canada (Baier and Robertson, 1965). It was designed to estimate PET in cold regions, where it is generally low. In this study, we found that annual PET estimates obtained with the BR method were low for cold regions, but high for tropical regions (Fig. 1). Consequently, GSET estimates obtained with the BR method for cold regions were also lower than estimates using the other methods for irrigated maize production (Fig. 2b). On the other hand, the BR-based GSET estimates were quite high for the Af, Am, Aw, Cwa and Cwb regions (Figs. 2b and 3b), which suggests that BR may be less suitable for these areas because it was initially developed and tested for cold regions. As for production, BR led to the highest estimate of total maize production for rainfed cultivation (Table 3). We attribute this to the lowest crop water stress estimated with BR (Fig. S4). Given that BR led to the largest overestimation of yields (Fig. 5b), crop water stress probably tended to be underestimated with this method for rainfed cultivation.

The H method was developed for semi-arid and arid regions (Hargreaves and Allen, 2003). It led to low annual PET estimates for arid regions in our study compared with the other PET methods, whereas the estimated annual PET was relatively high for tropical regions (Fig. 1). As a consequence, the GSET estimates were also small for arid regions, but quite high for Af, Am, Aw, Cwa and Cfb regions, where annual precipitation for both irrigated and rainfed maize cultivation is sufficiently high (Figs. 2–3). This implies that H tends to overestimate GSET in humid regions. The higher GSET

estimates for humid regions were consistent with findings by other studies Yoder et al. (2005), Trajkovic, (2007), and Saghraani et al. (2009). Trajkovic (2007) proposed an exponential index of 0.424 in Eq. (2) instead of 0.6 for humid regions. Moreover, using H led to the highest maize production estimates for irrigated cultivation (Table 3), which implies that H is likely to overestimate crop yields under sufficient water supplying conditions.

P was once recommended as the reference PET method by FAO (Doorenbos, 1977). However, it was replaced by PM, because it overestimated PET for a wide range of environmental conditions (Allen et al., 1998). Sau et al. (2004) even recommended to delete the P option from the DSSAT model because of its poor performance compared with other options in DSSAT. We also found that the estimates of annual PET and GSET obtained with the P method were higher than those obtained with PM method (Figs. 1–3). Considering the better agreement between estimated and reported yields with PM- than P-based PET estimates and that both require the same climate input data, we suggest to use PM instead of P in simulating maize growth on a global scale. Besides, the estimation of PPT with PM considers LAI and CO₂ in calculating canopy resistance coefficient for the whole crop growing period. This is one of major differences of PM from the other PET methods and could be part of the reason that PM performed more reliably for yield estimation. Therefore, if input data are not the major limitation, we recommend PM to be used for global crop simulation.

5. Conclusion

Large-scale crop models are major tools used to investigate the global water-food relations, the impacts of climate change on food production and irrigation demand, and to assess water management strategies for alleviating water scarcity and enhancing food security. This study demonstrates that different PET methods can lead to large uncertainties in the estimation of crop-water relations, which could impair sound decision making for policy makers.

The differences in annual PET estimates obtained with different PET methods were significant. Their impacts on predictions of water related variables (e.g. GSET, irrigation water requirement, and CWU) were more substantial than on yields. At the same time, also water availability played an important role for predictions of GSET and yields. Overall, PT tended to estimate high GSET and to underestimate yields. H and BR tended to estimate high GSET for rainfall sufficient regions. In rainfall-limited regions, all the PET methods performed consistently, except the overestimation of maize yield with BR due to its lower estimation of water stress. Globally, PM was more reliable in yield estimation than the other PET methods and has more reasonable implementation in estimating PPT by considering the effects of LAI and CO₂ on canopy resistance coefficient, thus should be considered with priority. However, PM requires more climate variables than H, BR, and PT. In contrast, H and BR only require temperature. However, BR tended to overestimate maize yield for rainfed cultivation, where H performed reasonably well for most regions except for high-rainfall regions. If obtaining whole set of climate data is a major challenge, H is a valid alternative option for all other regions except for high-rainfall regions.

Acknowledgements

This study was jointly supported by Eawag and World Food System Center at ETH Zürich. Christian Folberth was supported by a Research Fellowship of the Center for Advanced Studies of Ludwig Maximilian University, Munich. We would like to express our gratitude to Joshua Elliott of the GGCM Project and the ISI-MIP project coordinators for providing processed climate input data.

We are also grateful to two anonymous reviewers for their valuable comments to improve the quality of our paper.

Appendix A. Supplementary data

Supplementary data associated with this article can be found, in the online version, at <http://dx.doi.org/10.1016/j.agrformet.2016.02.017>.

References

- Allen, R.G., Pereira, L.S., Raes, D., Smith, M., 1998. Crop evapotranspiration – Guidelines for computing crop water requirements. FAO Irrigation and drainage paper 56. FAO, Rome.
- Anothai, J., Soler, C.M.T., Green, A., Trout, T.J., Hoogenboom, G., 2013. Evaluation of two evapotranspiration approaches simulated with the CSM–CERES–Maize model under different irrigation strategies and the impact on maize growth, development and soil moisture content for semi-arid conditions. *Agric. For. Meteorol.* 176, 64–76.
- Baier, W., Robertson, G.W., 1965. Estimation of latent evaporation from simple weather observations. *Can. J. Plant Sci.* 45 (3), 276–284.
- Balkovič, J., et al., 2013. Pan-European crop modelling with EPIC: implementation, up-scaling and regional crop yield validation. *Agrofor. Syst.* 120, 61–75.
- Balkovič, J., et al., 2014. Global wheat production potentials and management flexibility under the representative concentration pathways. *Global Planet. C* 122, 107–121.
- Bassu, S., et al., 2014. How do various maize crop models vary in their responses to climate change factors? *Global Change Biol.* 20 (7), 2301–2320.
- Batjes, N.H., 2006. ISRIC-WISE derived soil properties on a 5 by 5 arc-minutes global grid (version 1.1). ISRIC–World Soil Information, Wageningen.
- Benson, V., Potter, K., Bogusch, H., Goss, D., Williams, J., 1992. Nitrogen leaching sensitivity to evapotranspiration and soil water storage estimates in EPIC. *J. Soil Water Conserv.* 47 (4), 334–337.
- Chapagain, A.K., Hoekstra, A.Y., 2004. Water footprints of nations. Research Report Series No. 16. UNESCO-IHE, Delft.
- Doorenbos, J., 1977. Guidelines for predicting crop water requirements. *FAO Irrig. Drain. Pap.* 24, 15–29.
- Elliott, J., et al., 2014. Constraints and potentials of future irrigation water availability on agricultural production under climate change. *Proc. Natl. Acad. Sci. U. S. A.* 111 (9), 3239–3244.
- Elliott, J., et al., 2015. The global gridded crop model intercomparison: data and modeling protocols for phase 1 (v1.0). *Geosci. Model Dev.* 8 (2), 261–277.
- FAO, 1995. Digital Soil Map of the World Map. FAO, Rome.
- FAO, 2007. FertiSTAT—Fertilizer Use Statistics. FAO, Rome.
- Fader, M., et al., 2011. Internal and external green-blue agricultural water footprints of nations, and related water and land savings through trade. *Hydrol. Earth Syst. Sci.* 15 (5), 1641–1660.
- Folberth, C., Gaiser, T., Abbaspour, K.C., Schulin, R., Yang, H., 2012. Regionalization of a large-scale crop growth model for sub-Saharan Africa: model setup, evaluation, and estimation of maize yields. *Agric. Ecosyst. Environ.* 151, 21–33.
- Folberth, C., Yang, H., Gaiser, T., Abbaspour, K.C., Schulin, R., 2013. Modeling maize yield responses to improvement in nutrient, water and cultivar inputs in sub-Saharan Africa. *Agric. Syst.* 119, 22–34.
- Folberth, C., et al., 2014. Effects of ecological and conventional agricultural intensification practices on maize yields in sub-Saharan Africa under potential climate change. *Environ. Res. Lett.* 9 (4), 044004.
- Gassman, P.W. et al., 2005. Historical development and applications of the EPIC and APEX Models Iowa State University, Center for Agricultural and Rural Development. Working Paper 05-WP 397, Ames, Iowa.
- Hargreaves, G.H., Allen, R.G., 2003. History and evaluation of Hargreaves evapotranspiration equation. *J. Irrig. Drain. Eng.* 129 (1), 53–63.
- Hargreaves, G.H., Samani, Z.A., 1985. Reference crop evapotranspiration from temperature. *Appl. Eng. Agric.* 1 (2), 96–99.
- Hempel, S., Frieler, K., Warszawski, L., Schewe, J., Piontek, F., 2013. A trend-preserving bias correction – the ISI-MIP approach. *Earth Syst. Dyn.* 4 (2), 219–236.
- Jensen, M.E., Burman, R.D., Allen, R.G., 1990. Evapotranspiration and Irrigation Water Requirements. ASCE Manual of Practice No. 70. ASCE, New York.
- Jones, J.W., et al., 2003. The DSSAT cropping system model. *Eur. J. Agron.* 18 (3–4), 245–265.
- Kiniry, J.R., Williams, J.R., Gassman, P.W., Debaeke, P., 1992. A general, process-oriented model for two competing plant species. *Trans. ASABE* 35 (3), 801–810.
- Knisel, W.G., 1980. CREAMS: a field-scale model for chemicals, runoff and erosion from agricultural management systems. Conservation Research Report No. 26, Washington D.C.
- Leonard, R.A., Knisel, W.G., Still, D.A., 1987. GLEAMS: groundwater loading effects of agricultural management systems. *Trans. ASABE* 30 (5), 1403–1418.
- Liu, J., Williams, J.R., Zehnder, A.J.B., Yang, H., 2007. GEPIC—modelling wheat yield and crop water productivity with high resolution on a global scale. *Agric. Syst.* 94 (2), 478–493.
- Liu, J., Zehnder, A.J.B., Yang, H., 2009. Global consumptive water use for crop production: the importance of green water and virtual water. *Water Resour. Res.* 45 (5).
- Liu, J., et al., 2013. A global and spatially explicit assessment of climate change impacts on crop production and consumptive water use. *PLoS One* 8 (2), e57750.
- Liu, J., 2009. A GIS-based tool for modelling large-scale crop-water relations. *Environ. Modell. Software* 24 (3), 411–422.
- Mekonnen, M.M., Hoekstra, A.Y., 2011. The green, blue and grey water footprint of crops and derived crop products. *Hydrol. Earth Syst. Sci.* 15 (5), 1577–1600.
- Mitchell, T.D., Jones, P.D., 2005. An improved method of constructing a database of monthly climate observations and associated high-resolution grids. *Int. J. Climatol.* 25 (6), 693–712.
- Monteith, J., 1965. Evaporation and environment. *Symp. Soc. Exp. Biol.* 19, 205–234.
- Palosuo, T., et al., 2011. Simulation of winter wheat yield and its variability in different climates of Europe: a comparison of eight crop growth models. *Eur. J. Agron.* 35 (3), 103–114.
- Parton, W.J., et al., 1994. A general model for soil organic matter dynamics: sensitivity to litter chemistry, texture and management. *Soil Sci. Soc. Am. Inc., Minneap. Minn. U. S. A.*, 147–167.
- Peel, M.C., Finlayson, B.L., McMahon, T.A., 2007. Updated world map of the Köppen–Geiger climate classification. *Hydrol. Earth Syst. Sci.* 11 (5), 1633–1644.
- Penman, H.L., 1948. Natural evaporation from open water, bare soil and grass. *Proc. R. Soc. Lond. Ser. A* 193 (1032), 120–145.
- Portmann, F.T., Siebert, S., Doll, P., 2010. MIRCA2000 – Global monthly irrigated and rainfed crop areas around the year 2000: a new high-resolution data set for agricultural and hydrological modeling. *Global Biogeochem. Cycles*, 24.
- Priestley, C., Taylor, R., 1972. On the assessment of surface heat flux and evaporation using large-scale parameters. *Mon. Weather Rev.* 100 (2), 81–92.
- Ritchie, J.T., 1972. Model for predicting evaporation from a row crop with incomplete cover. *Water Resour. Res.* 8 (5), 1204–1213.
- Roloff, G., Jong, R.D., Zentner, R., Campbell, C., Benson, V., 1998. Estimating spring wheat yield variability with EPIC. *Can. J. Soil Sci.* 78 (3), 541–549.
- Rosenzweig, C., et al., 2013. The agricultural model intercomparison and improvement project (AgMIP): protocols and pilot studies. *Agric. For. Meteorol.* 170, 166–182.
- Rosenzweig, C., et al., 2014. Assessing agricultural risks of climate change in the 21st century in a global gridded crop model intercomparison. *Proc. Natl. Acad. Sci. U. S. A.* 111 (9), 3268–3273.
- Sacks, W.J., Deryng, D., Foley, J.A., Ramankutty, N., 2010. Crop planting dates: an analysis of global patterns. *Global Change Biol.* 19 (5), 607–620.
- Saghavani, S.R., Ari Mustapha, S., Ibrahim, S., Randjbaran, E., 2009. Comparison of daily and monthly results of three evapotranspiration models in tropical zone: a case study. *Am. J. Environ. Sci.* 5 (6), 698.
- Sau, F., Boote, K.J., Bostick, W.M., Jones, J.W., Minguez, M.I., 2004. Testing and improving evapotranspiration and soil water balance of the DSSAT crop models. *Agron. J.* 96 (5), 1243–1257.
- Shiklomanov, I.A., 2003. World Water Resources at the Beginning of the 21st Century. Cambridge University Press, Cambridge.
- Siebert, S., Döll, P., 2010. Quantifying blue and green virtual water contents in global crop production as well as potential production losses without irrigation. *J. Hydrol.* 384 (3–4), 198–217.
- Tan, G.X., Shibasaki, R., 2003. Global estimation of crop productivity and the impacts of global warming by GIS and EPIC integration. *Ecol. Modell.* 168 (3), 357–370.
- Trajkovic, S., 2007. Hargreaves versus Penman–Monteith under humid conditions. *J. Irrig. Drain. Eng.* 133 (1), 38–42.
- Wang, K.C., Dickinson, R.E., 2012. A review of global terrestrial evapotranspiration: observation, modeling climatology, and climatic variability. *Rev. Geophys.*, 50.
- Weedon, G.P., et al., 2014. The WFDEI meteorological forcing data set: WATCH forcing data methodology applied to ERA-Interim reanalysis data. *Water Resour. Res.* 50 (9), 7505–7514.
- Williams, J.R., Jones, C.A., Dyke, P.T., 1984. A modeling approach to determining the relationship between erosion and soil productivity. *Trans. ASABE* 27 (1), 129–144.
- Williams, J.R., 1995. The EPIC model. In: Singh, V.P. (Ed.), *Computer Models of Watershed Hydrology*. Water Resources Publications, Highlands Ranch, Colo.
- Xiong, W., et al., 2014. A calibration procedure to improve global rice yield simulations with EPIC. *Ecol. Modell.* 273, 128–139.
- Yin, Y.Y., et al., 2014. GEPIC-V-R model: a GIS-based tool for regional crop drought risk assessment. *Agric. Water Manage.* 144, 107–119.
- Yoder, R.E., Odhiambo, L.O., Wright, W.C., 2005. Evaluation of methods for estimating daily reference crop evapotranspiration at a site in the humid Southeast United States. *Appl. Eng. Agric.* 21 (2), 197–202.